

Electrochemical Deposition and Characterization of ZnO Nanowire Arrays with Tailored Dimensions

C. Lévy-Clément^a, J. Elias^a, R. Tena-Zaera^a, I. Mora-Sero^b, Y. Luo^b and J. Bisquert^b

^a Institut de Chimie et Matériaux de Paris-Est, CNRS, UMR 7182, 94320 Thiais, France

^b Departament de Física, Universitat Jaume I, 12071 Castelló, Spain

A systematic study of the deposition of single crystal ZnO nanowire arrays from the oxygen electroreduction was performed. The influence of deposition parameters such as the concentrations of zinc precursor (ZnCl₂) and supporting electrolyte (KCl) on the formation of ZnO nanowire arrays, as well as on the dimensions of the nanowires was analyzed. Mean nanowire diameters from 25 to 80 nm were obtained by only modifying the [ZnCl₂] in solution, while high [KCl] allowed to reach diameters as high as 300 nm. The influence of [KCl] on the donor density determined from electrochemical impedance spectroscopy of ZnO nanowires was also shown. Carrier densities from 10¹⁷ to 10²⁰ cm⁻³ were obtained depending on the deposition and annealing conditions. The results show that electrodeposition is a cost-effective technique which allows not only to grow ZnO single crystal nanowire arrays with tailored dimensions, but also to act on their electrical properties in a controlled way.

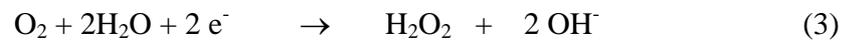
Introduction

Single-crystal ZnO nanowire arrays have attracted a lot of research interest in recent years because they may be used as building blocks for a new generation of devices in different technological domains such as optoelectronics (1, 2), solar cells (3, 4), gas sensing (5), field emission (6, 7) and piezoelectrics (8). Present results confirm fairly well the multifunctional capabilities of ZnO nanowire arrays. However, more research is required to gain further insight into the fundamental mechanisms involved in the devices based on ZnO nanowires, and consequently, to increase their performance. In this framework, deposition of ZnO nanowire arrays with tailored dimensions and study of their electrical properties seem to be crucial.

With respect to deposition methods, until now most of the work has been focused on vapor phase techniques such as simple physical vapor deposition (9), metal-organic vapor phase epitaxy (10), chemical vapor transport and condensation (11). However, a method in solution such as electrodeposition not only appears as a low temperature alternative, well suited for cheap large-scale production of ZnO nanowire arrays.

Electrodeposition of ZnO is generally based on the generation of hydroxide ions (OH⁻) at the surface of a conducting electrode by cathodic reduction of a precursor such as nitrate ions (NO₃⁻) (12) or molecular oxygen (O₂) (13). The electroreduction of NO₃⁻ ion is a rather intricate process with many reactions probably involved in the process (14). Even in the most simplified interpretation (12), reduction of nitrate leads to some byproducts such as NO₂⁻ (eq. 1) that could induce some instabilities in ZnO deposition. Although the electroreduction of O₂ can take place by two different reaction pathways i.e.

four-electron (eq. 2) or two-electron processes (eq. 3) as a function of the electrolyte and cathode properties (15), it appears as a simple and attractive process to deposit ZnO under well controlled conditions. Pauporté et al. (16) have also studied the possibilities of using hydrogen peroxide (H₂O₂) as a direct source of OH⁻ ions (eq. 4). H₂O₂ is especially interesting to deposit thick layers because it presents a high solubility in water and, therefore, it allows achieving high deposition rates (17). Molecular O₂ has been the most frequently used in the deposition of ZnO nanowire arrays (18, 19). The promising capabilities of these nanostructures to develop electronic devices such as hybrid light emitting diodes (2) and nanostructured solar cells (3) have already been shown.



Nevertheless, the electrodeposition capabilities for tailoring ZnO nanowire dimensions have not yet been fully exploited. Leprince-Wang et al (20) have attempted to control the nanowire diameter by using commercial porous polycarbonate membranes. They observed an important difference (> 60%) between the obtained nanowire diameters and the nominal pore diameter of the membranes. In addition, the structural and surface properties of electrodeposited ZnO nanowires strongly depend on the quality of the host wall pores. The presence of defects in pore walls may result in polycrystalline ZnO nanowires (21). Thus, template-free electrochemical methods appear to be an advantageous option. Our previous study has shown that the use of a ZnO buffer layer constituted of crystallites of well controlled size can be an efficient way to act on the diameter of ZnO nanowires and on their density in the array (22). On the other hand, Xu et al. (23) recently suggested the possible role of Cl⁻ ions as adsorbent species to stabilize some ZnO faces, and therefore, to hind the growth along the corresponding direction. Nevertheless, they have not investigated this strategy to control the ZnO nanowire dimensions in the arrays.

The use of inorganic ions as selective ZnO face stabilizers appears as a very interesting alternative to organic capping agents (24, 25) because it may also be an efficient strategy to act on the electrical properties of ZnO nanowires. Similar ways have been theoretically studied to attempt the doping in semiconductor crystals (26). However, the particular morphology of nanowire arrays makes their electrical characterization difficult by using standard solid-state techniques. In contrast, by establishing a semiconductor/liquid junction it is possible to investigate the electrical properties of nanowire arrays using standard electrochemical methods such as impedance spectroscopy. A cylindrical Mott-Schottky (MS) model has been recently developed to determine the carrier density in ZnO nanowire arrays (27).

Here, we present a systematic study of the effect of zinc precursor (ZnCl₂) and supporting electrolyte (KCl) concentrations on the deposition of ZnO nanowire arrays from the molecular oxygen electroreduction. The influence of both parameters on nanowire dimensions is emphasized. The effect of the KCl concentration on the carrier density of ZnO nanowires is also discussed, showing that it is a major parameter not only to control the ZnO nanowire dimensions, but also their electrical properties.

Experimental

The electrodeposition of ZnO was performed in a three-electrode electrochemical cell with the substrate (conducting glass) as the cathode, a Pt spiral wire as the counter electrode and a Saturated Calomel Electrode (SCE) as the reference electrode. The electrolyte was an aqueous solution of ZnCl₂ and KCl, saturated with bubbling oxygen. The ultrapure water (18 MΩ·cm) was provided by a Millipore setup. The ZnCl₂ salt (Flucka, purity > 98.0 %) acts as a Zn²⁺ precursor and its concentration was varied from 5x10⁻⁵ to 5x10⁻³ M. While, KCl (Flucka, purity > 99.5 %) acts, among other roles, as a supporting electrolyte. Its concentration was in the 5x10⁻² to 4 M range.

The substrates were commercial conducting (10 Ω/square) glass/SnO₂:F from Asahi Glass Company. As a first step, they were covered by a nanocrystalline ZnO buffer layer that was galvanostatically ($J = 0.15 \text{ mA/cm}^2$) electrodeposited using ZnCl₂ and KCl concentrations of 5x10⁻³ and 0.1 M, respectively. Then, on top of the nanocrystalline ZnO buffer layer, the ZnO nanowire arrays were electrodeposited under a constant potential (-1 V versus SCE). The deposition temperature was 25°C for the buffer layer and 80°C for the nanowire arrays. The charge density was 0.4 and 20 C/cm² for the first and second cases, respectively.

Cyclic voltammetry (CV) experiments were performed at 80°C. Two scans for each cathode were carried out from solution rest potential (near zero), with a cathodic sweep to -1.5 V vs. SCE and then an anodic sweep to +0.5 V vs. SCE. Scan rate was 10 mV/s.

Electrochemical impedance spectroscopy (EIS) measurements were performed in a three-electrode cell using a Pt wire as counter electrode and a standard Ag/AgCl in 3M KCl as reference electrode. A carbonate propylene electrolyte (0.1 M LiClO₄) was used to avoid ZnO decomposition. Each measurement was done applying a 20 mV AC sinusoidal signal over the constant applied bias with the frequency ranging between 500 kHz and 5 mHz. After the electrochemical measurement, the as-grown samples were annealed in air at 450°C for 1 hr at atmospheric pressure, followed by cooling in ambient air. Note that ZnO nanowire arrays analyzed by EIS were deposited on a sprayed ZnO buffer layer as in our previous studies (3, 19). Electrodeposition, CV experiments and EIS data were obtained using an Autolab PGSTAT-30 with a frequency analyzer (FRA) in the case of EIS.

Results and Discussion

Morphology of ZnO nanowire arrays

Our previous study showed that a ZnO buffer layer can be used to act on the diameter of ZnO nanowires and their density in the array (22). To expand the possibilities of free-template electrodeposition, the influence of concentrations of ZnCl₂ ([ZnCl₂]) and KCl ([KCl]) on nanowire dimensions has been analyzed.

ZnCl₂ concentration effects. In order to study the influence of [ZnCl₂] on the growth of ZnO nanowire arrays, their morphology was analyzed for different concentrations in the 5x10⁻⁵-1x10⁻³ M range.

The electrodeposition of nanowires was performed on the nanocrystalline ZnO buffer layer, the electrochemical parameters being hold constant ($V = -1.0 \text{ V vs SCE}$, $[KCl] =$

0.1 M, $T = 80^{\circ}\text{C}$ and $Q = 20\text{C}/\text{cm}^2$), except for $[\text{ZnCl}_2]$. For $[\text{ZnCl}_2]$ lower than 5×10^{-5} M, no ZnO deposition was obtained. $[\text{ZnCl}_2]$ greater than 1×10^{-3} M resulted in close-packed, thick (> 200 nm) vertical nanorods that constituted a compact ZnO layer, without however exceeding 1×10^{-2} M that promotes the deposition of zinc hydroxychloride (13).

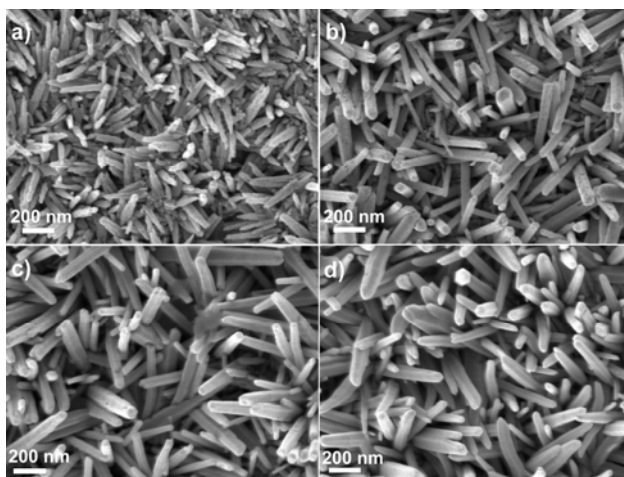


Figure 1. Plan view SEM images of ZnO nanowire arrays electrodeposited using different ZnCl_2 concentrations: a) 5×10^{-5} M, b) 1×10^{-4} M, c) 5×10^{-4} M and d) 1×10^{-3} M.

Figure 1 shows that the nanowire diameter increases with $[\text{ZnCl}_2]$. This is not surprising because an increase of particle size is generally expected, in solution techniques, when the precursor concentration increases (28, 29). Nevertheless, to gain a further insight into the diameter variation, average values were calculated from a statistical analysis of the SEM images. The average diameter evolution as a function of ZnCl_2 is summarized in Fig. 2, underlining that the nanowire diameter is more sensitive to $[\text{ZnCl}_2]$ at low ($< 5 \times 10^{-4}$ M) than at high concentrations. Apparently, for the lowest $[\text{ZnCl}_2]$ the most important part of Zn^{2+} reacts with OH^- ions adsorbed on the nanowire tips because they are more easily accessible. The lateral growth of nanowires is very slow, resulting in thin nanowires of ~ 25 nm in diameter that matches considerably with the crystallite size of nanocrystalline ZnO buffer layer (22). As $[\text{ZnCl}_2]$ increases, there are not enough OH^- ions adsorbed on the nanowire tips to react with all Zn^{2+} ions close to them, promoting an increase of Zn^{2+} concentration around the entire nanowire surface, enhancing the lateral growth. The increase of $[\text{Zn}^{2+}]/[\text{OH}^-]$ ratio smoothes the effect of $[\text{ZnCl}_2]$ on the nanowire diameter, as can be observed for high $[\text{ZnCl}_2]$ values (higher than 5×10^{-4} M). We can conclude that the ZnO nanowire growth is mainly limited by Zn^{2+} ions in the low $[\text{ZnCl}_2]$ regime. As $[\text{ZnCl}_2]$ increases, the oxygen reduction becomes important, being probably determined by the preferential adsorption of OH^- ions on (0001) ZnO face due to its polar nature (30). The nanowire length was measured from cross section SEM images (not shown here). A similar behavior of the variation of $[\text{ZnCl}_2]$ on the nanowire diameter was also observed for the length. This similarity supports the above discussion.

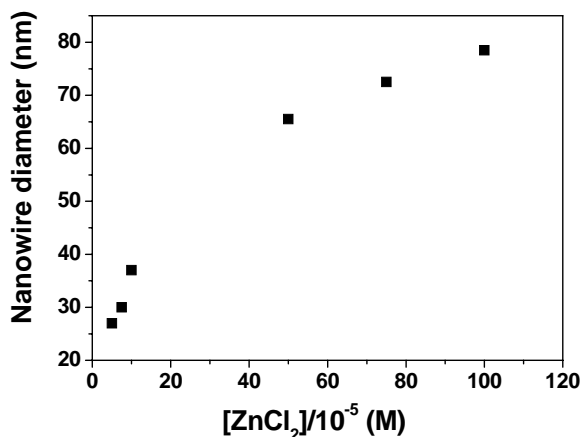


Figure 2. Nanowire diameter as a function of ZnCl₂ concentration.

With respect to the density of nanowire arrays, Fig. 1 shows that the lowest packing corresponds to the highest ZnCl₂ concentration (1×10^{-3} M). Although precursor concentration is a major parameter in nucleation step of solution methods (28, 29), other electrodeposition parameters (besides [ZnCl₂]) must be considered for analyzing the nanowire density trend. All samples of Fig. 1 were deposited using a charge density of 20 C/cm². This implies that the amount of OH⁻ ions produced during the deposition process is the same for all samples. Nevertheless, the ZnO amount may be different because the Zn²⁺ precursor concentration varies from one sample to other. As discussed before, the samples electrodeposited from more concentrated ZnCl₂ solutions result in longer nanowires. The differences in nanowire length could also contribute to the differences in array density. To check this point we electrodeposited several samples with [ZnCl₂] = 5×10^{-4} M using different charge densities. We observed that the nanowire density decreases with the length of individual nanowires, especially for values lower than 500 nm. This observation suggests that there is a selective process during nanowire growth. Likely the growth of the best vertically oriented nanowires is preferred because the Zn²⁺ ions react with the OH⁻ ions adsorbed on their top faces, while the Zn²⁺ ions do not reach the tips of the more inclined nanowires, quenching their growth. Otherwise, the deposition efficiency, defined as the ratio between the OH⁻ that reacted with Zn²⁺ and total amount of OH⁻, was very low (the highest one corresponds to [ZnCl₂] = 1×10^{-3} M and is < 2 %). This could be induced by a poor Zn²⁺ transport in the solution. To gain a further insight into this phenomenon the role of KCl concentration is analyzed in the next section. KCl, may act as a supporting electrolyte, determining the ionic conductivity of the solution. However, it can also act on the oxygen reduction due to high adsorption of Cl⁻ on the cathode surface, being in competition with OH⁻ adsorption.

KCl concentration effects. ZnO nanowire arrays were electrodeposited on ZnO nanocrystalline buffer layers, varying the KCl concentration from 0.05 to 4 M. The remaining electrochemical parameters were held constant ($V = -1.0$ V vs SCE, [ZnCl₂] = 5×10^{-4} M, $T = 80$ °C and $Q = 20$ C/cm²).

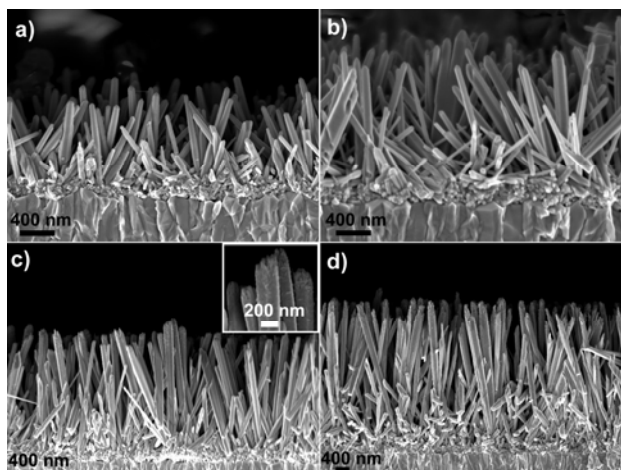


Figure 3. Cross section SEM images of ZnO nanowire arrays electrodeposited using different KCl concentrations: a) 0.05 M, b) 1 M, c) 2 M and d) 4M. Inset of Fig. 3c shows a high magnification image of ZnO nanowire tips.

Fig. 3 shows SEM cross section images of ZnO nanowire arrays obtained with different [KCl] values. Note that the bar scale length is different for figures 3a,b and 3c,d. A jump in nanowire diameter for concentrations higher than 1 M is clearly observed. From plan view SEM images (not show here), a mean diameter value in the range of 80-100 nm was estimated for samples electrodeposited for $[KCl] \leq 1$ M, while $[KCl] > 1$ M resulted in larger mean diameters up to 300 nm. This observation agrees with the role proposed by Xu et al. (23) for Cl^- as a stabilizer of (0001) ZnO faces. Nevertheless, taking into account that preliminary structural characterization showed that ZnO nanowires grow along (0001) direction (31), the expected hint of growth along the c-axis is not observed in our case. In fact, nanowire length increases with [KCl] (Fig.4).

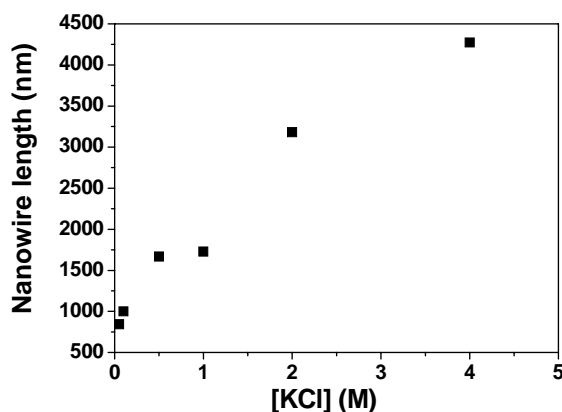


Figure 4. Nanowire length as a function of KCl concentration.

In order to gain a further insight into the mechanism that promotes the variation of nanowire length, the current density was dynamically analyzed during the electrodeposition process for different KCl concentrations (Fig. 5).

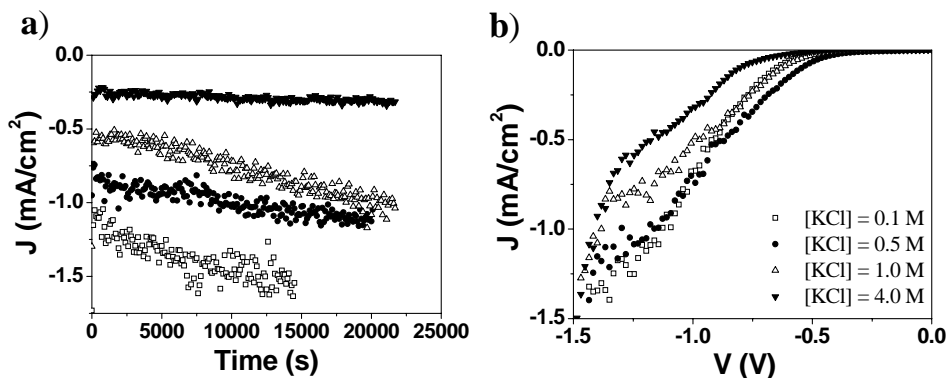


Figure 5. a) Current density during ZnO nanowire array electrodeposition and b) cathodic current-potential scans on SnO₂:F electrode for different KCl concentrations. The legend is the same for both figures.

Fig. 5a shows a clear decrease of the current density when [KCl] increases. This may indicate that the electroreduction of O₂ takes place more slowly. In other words, the time necessary to reduce the same amount of O₂ augments with [KCl] (Fig. 5a). This could be due not only to differences in the mechanism of O₂ electroreduction, but also to the modification of the electrode surface due to the ZnO nanowire growth. To exclude the latter point, CV scans were performed on conducting glass substrates in solutions with different KCl concentrations. Only the cathodic forward sweeps of second CV scan are shown in Fig. 5b for the sake of clarity. The second scan was chosen because the ZnO deposition may cover the SnO₂:F surface during the first CV scan. Then, the second scan is more representative of the O₂ reduction process during the ZnO nanowire deposition, which was performed on ZnO buffer layers.

Fig. 5b reveals that even on flat cathodes the current density decreases when [KCl] increases, pointing out that KCl concentration appears as the major parameter in the current decrease. This could be due to a competition of adsorption between OH⁻ and Cl⁻ on cathode surface. Other authors found that the presence of Cl⁻ modifies the oxygen reduction mechanism on metallic substrates such as silver (32) and nickel (33), inducing the formation of H₂O₂ as an intermediate species by a two-electron reduction process (eq. 3). A similar phenomenon may also occur in our electrodeposition experiments. Goux et al. (34) have recently studied the O₂ electroreduction on ZnO electrodes. Unfortunately, they did not report the influence of [KCl] on the process and a direct comparison with our results cannot be fully established. However, they found that for [KCl] = 0.1 M that the total number of exchanged electrons during O₂ reduction is ~ 3.2. This may indicate that a four-electron process is dominant under these conditions. Nevertheless, the two-electron process may become more important when [KCl] increases as observed on metal cathodes (32, 33).

As already discussed, the ZnO deposition efficiency was very low for 0.1 M. KCl. It increases as a function of [KCl] and an efficiency of ~ 15 % was roughly estimated for ZnO nanowire arrays deposited using the highest KCl concentration (4 M). Higher deposition efficiencies could also be obtained using a bigger electrochemical cell, because in the present case the ZnO deposition was limited by the total amount of Zn²⁺

inside the used cell. The lack of Zn^{2+} induced some growth discontinuities at the end of electrodeposition experiments with $[\text{KCl}]$ as high as 2 and 4 M, promoting some defects on nanowire tips (Inset of Fig. 3c).

As a partial summary, playing with KCl concentration appears to be an efficient way to act on O_2 reduction rate. This results in an increase of the efficiency of ZnO deposition process; and therefore, in longer nanowires while generating the same amount of OH^- ions. This is the major role played by the concentration of KCl on the electrodeposition of ZnO nanowire arrays from O_2 reduction. A considerable increase of ZnO nanowire diameter was also observed for high $[\text{KCl}]$ (>1 M). This can be due to the stabilization of top face of nanowires due to a selective Cl^- adsorption on (0001) ZnO face. Cl^- ions adsorbed ions may also act on the electrical properties of ZnO nanowires. In this framework, EIS study was performed to analyze the effects.

Electrical properties of ZnO nanowire arrays

A Mott-Schottky (MS) model, taking into account the particular morphology of nanowire arrays, has been recently developed to determine the carrier density in electrodeposited ZnO samples. The details of the model can be found elsewhere (27). Here, we only discuss the evolution of the donor density as a function of $[\text{KCl}]$ in solution. Fig. 6 summarizes the donor density of electrodeposited ZnO nanowires for as deposited samples and those annealed in air at 450°C for 1 hour.

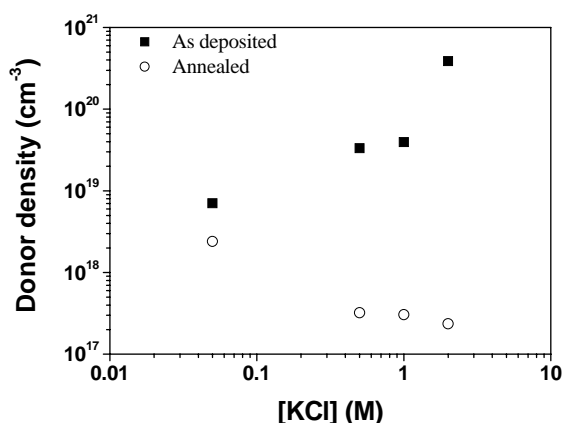


Figure 6. Donor density of ZnO nanowires as a function of KCl concentration.

For the as deposited samples, the donor density increases as a function of $[\text{KCl}]$. On the contrary, after annealing, the donor density decreases with $[\text{KCl}]$. Variations in donor densities from 10^{17} to 10^{20} cm^{-3} were obtained as a function of the deposition and annealing conditions. This indicates that $[\text{KCl}]$ plays a major role not only on ZnO nanowire dimensions, but also on their electrical properties.

As preliminary comments, we would like to note that the increase of $[\text{KCl}]$ may result not only in a higher adsorption of Cl^- on ZnO nanowires, but also in an increase of the $[\text{Zn}^{2+}]/[\text{OH}^-]$ ratio close to the cathode. Since the energy formation of ZnO intrinsic defects with an electrical donor behavior, such as oxygen vacancies (V_O) or zinc atoms in interstitials positions (Zn_i) decreases in zinc rich conditions (35, 36), the increase of the $[\text{Zn}^{2+}]/[\text{OH}^-]$ ratio may result in a higher amount of donor defects in ZnO nanowires. This

could explain the increase of donor density as a function of [KCl] in the as deposited samples. The concentration of intrinsic donor defects (especially V_O) should decrease after annealing in air, giving more relevance to the electrical role of Cl atoms placed in ZnO lattice. If Cl atoms are placed in interstitial positions they may play an electrical role as charge-acceptors, inducing some compensation effects. A stronger compensation due to a higher concentration of Cl atoms could be the origin of the decrease of the donor density with [KCl] increase for air annealed samples.

However, this is only a possibility and other situations cannot be excluded. Some structural characterization is now undertaken to gain a further insight into the position of Cl atoms in ZnO lattice because it may be crucial for their electrical behavior.

Conclusions

A systematic study of the role of $ZnCl_2$ and KCl concentration on the deposition of ZnO nanowire arrays from oxygen electroreduction is reported. The variation of $[ZnCl_2]$ appears as an efficient way to control the ZnO nanowire diameter. Meanwhile, the [KCl] not only acts on the diameter of nanowires, but also plays a major role on their growth rate. This is discussed in the frame of the differences induced by Cl^- ions in the O_2 reduction mechanism. The carrier density of electrodeposited ZnO nanowires was determined from electrochemical impedance spectroscopy by using a cylindrical Mott-Schottky model. Carrier densities from 10^{17} to 10^{20} cm^{-3} have been obtained as a function of the KCl concentration and annealing conditions. This work not only shows the high potentiality of the electrochemical techniques in the deposition of ZnO nanowire arrays with tailored dimensions, but also in the study of their electrical properties.

References

1. W.I. Park, G.C. Yi, *Adv. Mater.* **16**, 87 (2004).
2. R. Konenkamp, R. C. Word, and M. Godinez, *Nano Letters*, **5**, 2005 (2005).
3. C. Lévy-Clément, R. Tena-Zaera, M. A. Ryan, A. Katty, G. Hodes, *Adv. Mater.*, **17**, 17, 1512 (2005).
4. M. Law, L.E. Greene, J.C. Johnson, R. Saykally, P. Yang, *Nature Mater.*, **4**, 455 (2005).
5. L.C. Tien, P.W. Sadik, D.P. Norton, L.F. Voss, S.J. Pearton, H.T. Wang, B.S. Kang, F. Ren, J. Jun, J. Lin, *Appl. Phys. Lett.*, **87**, 222106 (2005).
6. Y.K. Tseng, C.J. Huang, H.M. Cheng, I.N. Lin, K.S. Liu, I.C. Chen, *Adv. Funct. Mater.*, **13**, 811 (2003).
7. S.Y. Li, P. Lin, C.Y. Lee, T.Y. Tseng, *J. Appl. Phys.*, **95**, 3711 (2004).
8. Z.L. Wang, J. Song, *Science*, **312**, 242 (2006).
9. S.C. Lyu, Y. Zhang, C.J. Lee, *Chem. Mater.*, **15**, 3294 (2003).
10. W.I. Park, D.H. Kim, S.W. Jung, G.C. Yi, *Appl. Phys. Lett.*, **80**, 4232 (2002).
11. P. Yang, H. Yan, S. Mao, R. Russo, J. Johnson, R. Saykally, N. Morris, J. Pham, R. He, H.J. Choi, *Adv. Funct. Mat.*, **12**, 323 (2002).
12. M. Izaki, T. Omi, *J. Electrochem. Soc.*, **143**, L53 (1996).
13. S. Peulon, D. Lincot, *J. Electrochem. Soc.*, **145**, 864 (1998).
14. W.J. Plieth, *Encyclopedia of Electrochemistry of the Elements*, A. J. Bard, Editors, vol. 8, chapter 5, Marcel Dekker, New York (1978).
15. S. Strbac, R. R. Adzic, *Electrochim. Acta*, **41**, 2903 (1996).
16. Th. Pauporté, D. Lincot, *J. Electroanal. Chem.* **517**, 54 (2001).

ECS Transactions 6, 405 (2007)

17. Th. Pauporté, D. Lincot, *J. Electrochem. Soc.* **148**, C310 (2001).
18. R. Könenkamp, K. Boedecker, M.C. Lux-Steiner, M. Poschenrieder, F. Zenia, C.Lévy-Clément, S. Wagner, *Appl. Phys. Lett.* **77**, 2575 (2000).
19. R. Tena-Zaera, A. Katty, S. Bastide, C. Lévy-Clément, B. O'Regan, V. Muñoz-Sanjosé, *Thin Solid Films*, **483**, 372 (2005).
20. Y. Leprince-Wang, G.Y. Wang, X.Z. Zhang, D.P. Yu, *J. Cryst. Growth* **287**, 89 (2006).
21. M.J. Zheng, L.D. Zhang, G.H. Li, W.Z. Shen, *Chem. Phys. Lett.* **363**, 123 (2002).
22. J. Elias, R. Tena-Zaera, C. Lévy-Clément, *Thin Solid Films*, in press.
23. L. Xu, Y. Guo, Q. Liao, J. Zhang, D. Xu, *J. Phys. Chem. B* **109**, 13519 (2005).
24. E. Michaelis, D. Wöhrle, J. Rathousky, M. Wark, *Thin Solid Films*, **497**, 163 (2006).
25. Z. Chen, Y. Tang, C. Zhang, Y. Luo, *Electrochim. Acta*, **51**, 5873 (2006).
26. S.C. Erwin, L. Zu, M. I. Haftel, A.L. Efros, T.A. Kennedy, D. J. Norris, *Nature*, **436**, 91 (2005).
27. I. Mora-Sero, F. Fabregat-Santiago, B. Denier, J. Bisquert, R. Tena-Zaera, J. Elias, C. Lévy-Clément, *Appl. Phys. Lett.*, **89**, 203117 (2006).
28. G. Hodes, *Chemical Deposition of Semiconductor Films*, Marcel Dekker, Inc., New York and Basel (2003).
29. C. Burda, X. Chen, R. Narayanan, M.A. El-Sayed, *Chem. Rev.*, **105**, 1025 (2005).
30. A. Wander, N.M. Harrison, *J. Chem. Phys.* **115**, 2312 (2001).
31. C. Lévy-Clément, J. Elias, R. Tena-Zaera, SPIE Proceeding Series, Vol. 6340, Solar Hydrogen and Nanotechnology, L. Vayssières Ed., 63 400R (2006).
32. E. Brandt, *J. Electroanal. Chem.*, **150**, 97 (1983).
33. S.P. Jiang, C.Q. Cui, A.C.C. Tseung, *J. Electrochem. Soc.* **138**, 3599 (1992).
34. A. Goux, T. Pauporté, D. Lincot, *Electrochim. Acta*, **51** 3168 (2006).
35. S.B. Zhang, S.H. Wei, A. Zunger, *Phys. Rev. B*, **63**, 75205 (2003).
36. A.F. Kohan, G. Ceder, D. Morgan, C.G. Van de Walle, *Phys. Rev. B*, **61** 15019 (2000).